

Preparation of Nano-DAAF Explosive with Improved Initiation Sensitivity

Jun Wang,*^[a] Yanyang Qu,^[a] Yao Wang,^[a] Long Zhang,^[a] and Zhiqiang Qiao^[a]

Abstract: 3,3'-diamino-4,4'-zoxofurazan (DAAF) shows fascinating properties and can be practically applied in explosives and solid rocket propellants. Nano-sized DAAF explosive particles were prepared by a low-temperature and rapid crystallization process to improve energetic performance. The diameter and morphology of DAAF nanoparticles were characterized by Field emission scanning electron microscopy (FE-SEM), Atomic force microscopy (AFM) and X-ray diffraction (XRD). Nano-DAAF shows irregular spherical nano-particles with the diameter ranging from 50 to

100 nm. The size and morphology of nano-DAAF particles can be tuned by temperature difference and DAAF concentration of crystallization process. The thermal properties were also investigated by Differential scanning calorimetry (DSC). For nano-sized DAAF shows significantly decreased exothermal peak (259.3 °C) and enhanced energy release rate. Deflagration and short impulse shock waves experiments illustrated that nano-DAAF explosive shows significantly improved initiation sensitivity compared to micro-particles.

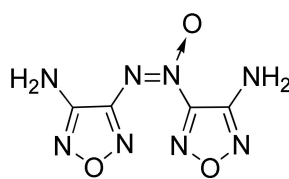
Keywords: nano-explosive · DAAF · preparation · spherical nano-particles · initiation sensitivity

1 Introduction

Furazan-based organic materials have been extensively studied and considered to be one of the most important class of energetic compounds due to their favorable properties such as high energy density, good safety, and high percentage of nitrogen content [1–3]. As a typical energetic furazan compounds, 3,3'-diamino-4,4'-zoxofurazan (DAAF) displays fascinating properties and can be practically applied in explosives and solid rocket propellants [4, 5]. The molecular structure of DAAF is illustrated in Scheme 1. Detonation pressure (31 GPa), detonation velocity (8.0 km s⁻¹) and critical diameter (<3 mm) of DAAF are better than 1,3,5-triamino-2,4,6-trinitrobenzene (TATB), which is standard of insensitive high explosives. The safety of DAAF and TATB is same level and cannot be initiated by laboratory impact drop tests [6, 7]. According to references [8–10], DAAF have provided the opportunity to develop insensitive high explosives and applied in advanced initiating devices and weapons with high safety.

Morphology and particle size of explosives play significant roles in the ignition, combustion and detonation performances. As it is known, nano materials have unique

large surface area and extraordinary properties due to great difference of the structures, sizes and shapes at the atomic and molecular scale [11, 12]. The use of nanotechnology to prepare nanostructure has provided a great approach to improve and optimize the properties of explosives. Nano-structured explosives have been attracted considerable interest for improving their performances in safety, ignition and detonation properties, and potential applications [13, 14]. It was reported that nano-explosives not only can decrease the mechanical sensitivity, but also help for improving the combustion and initiation properties as compared to coarse energetic materials. Nano-TATB was prepared by solvent/non-solvent recrystallization with concentrated sulfuric acid as solvent and water as non-solvent. The thermal decomposition takes place at lower temperature [15]. Y. Li prepared spherical TATB grains with the grain size from 40 to 50 nm by using solvent and non-solvent method, and spherical TATB grains had better heat resisting evenness and its 5 seconds ignition point is advanced by 7.5 K [16]. J. Wang reported on twin-fluid nozzle assisted precipitation (PTFN-P) to prepare nano-crystalline HNS with a crystal size of 120 ± 30 nm to reduce the sensitivity [17, 18]. Zhang prepared sub-micrometer-sized 2,6-diamino-3,5-dinitropyrazine-1-oxide (LLM-105) crystals by spray crystallization method, and it is more insensitive than micro-particle, under impact stimulus with a drop height (H₅₀) of 102 cm and short impulse shock wave [19]. D. Richardson investigated the sensitivity of hexanitrostilbene (HNS) to fly-



Scheme 1. Molecular structure of DAAF.

[a] J. Wang, Y. Qu, Y. Wang, L. Zhang, Z. Qiao

Institute of Chemical Materials, CAEP, Mianyang 621999, China

*e-mail: wjun927@caep.cn

er plate impact over a wide range of specific surface area (SSA). The result shown maximum sensitivity was found to occur at SSA between 10 and 20 m^2g^{-1} for HNS pressed to 90% theoretical maximum density [20]. Preparation of nano-explosives has been developed as effective way to decrease the mechanical sensitivity and improve the combustion and initiation properties. Therefore, it is necessary to develop facile methods to prepare nano-DAAF explosives to improve initiation properties for applications.

Considering all the above, we studied the preparation of nano-DAAF through introduced a rapid and low-temperature crystallization method. The morphology and size of nano-particles were tuned by temperature difference between solvent and water in crystallization process. The size and morphology were characterized by FE-SEM, AFM and XRD. The thermal property of nano-DAAF was illustrated by DSC and TG (thermogravimetry and differential scanning calorimetry). The research results reveal that nano-DAAF was successfully prepared and show significantly decreased exothermal peak and improved sensitivity for deflagration.

2 Experimental Section

Preparation process of nano-DAAF. Nano-DAAF particles were prepared by rapid and low-temperature crystallization process. In a typical experiment, 2.0 g of DAAF was dissolved in 10 ml of DMF (Dimethylformamide) at high temperature (20, 30, 40, 60 °C) for 10 min with magnetic stirring to form a red solution. This red solution was filtered to remove any suspended material. The filtrate was again heated to high temperature to dissolve the contents completely. The red solution was transferred to a crystallization instrument. Water as antisolvent was stirred at 1000 rpm at low temperature (2 °C). The red solution was sprayed into water for rapid crystallization to form nano-DAAF in solution and water. Nano-DAAF was separated. Then, the samples were collected and dried by freeze drying technology. Influence of experimental parameters such as temperature and concentration on the particle size of DAAF was studied.

Characterization. The morphologies of the samples were analyzed by field emission scanning electron microscopy (FE-SEM, Ultra 55) with an accelerating voltage of 6 kV. The nanoparticle size distribution of DAAF was calculated by means of counting more than 500 particles from the obtained SEM images via the statistics of the smileview software. The as-prepared samples were characterized by powder X-ray diffraction (XRD) using an X'Pert PRO X-ray diffractometer. The specific surface areas were measured by N_2 adsorption/desorption isotherms at 120 °C for 3 h using a Brunauer-Emmett-Teller (BET) analyzer of micromeritics ASAP 2020. The DSC was carried out from 100 °C to 400 °C at a rate of 10 °C/min under 50 ml/min N_2 flow.

The short duration pulse initiation sensitivity of the initiating explosive based on nano-DAAF was tested by means of a slapper detonator. The initiation threshold, expressed

as initiation voltage or initiation current of the capacitor discharge unit, flyer velocity was used to judge the initiation ability of nano-DAAF. The detailed experimental process was described in the literature [19,21].

3 Results and Discussion

DAAF nanoparticles were successfully prepared in this work by a rapid and low-temperature crystallization process. The morphology and size of the as-prepared samples were revealed by field-emission scanning electron microscopy (FE-SEM) and atomic force microscope (AFM). SEM image (Figure 1a) shows rodlike raw-DAAF with an average diameter of 500 nm and a length of 1–2 μm . Compared with raw-DAAF, AFM and SEM result clearly reveal that the DAAF particles have the shape of near spheres with the diameter ranging from 60 to 100 nm. As shown in Figure 1(c), nano-DAAF tend to agglomerate due to nano-DAAF particles have a high surface energy. Fortunately, the agglomerates of nano-DAAF can be dispersed into separate single particles (Figure 1b). The average size and particle size distribution of nano-DAAF were also calculated by means of counting more than 500 particles from the obtained SEM images via the statistics of the smile view software. Figure 1(d) shows the average particle size ranging 70 nm from 90 nm. Moreover, its particle size distribution is relatively narrow. The specific surface area of nano-DAAF is 16.3 m^2g^{-1} tested by N_2 adsorption/desorption isotherm, which shows a significantly increased of nano-DAAF compared with raw-DAAF with specific surface area of 3.8 m^2g^{-1} . Those results illustrate that nano-DAAF can be prepared by the rapid and low-temperature crystallization method.

The structure of raw-DAAF and nano-DAAF was further illustrated by XRD patterns (Figure 2). The peaks observed

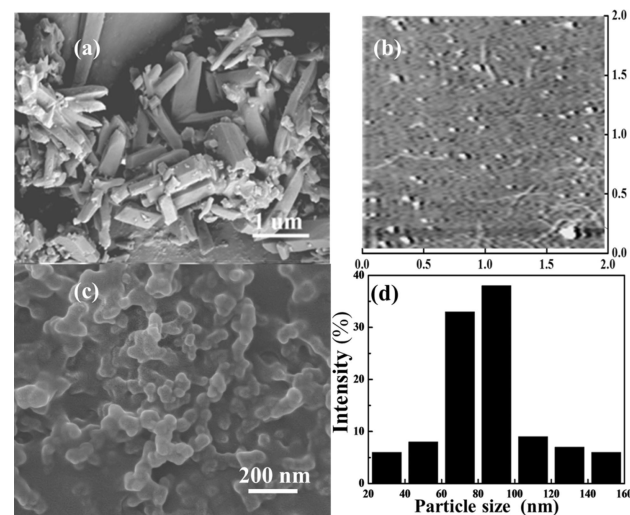


Figure 1. SEM, AFM and size distribution images of nano-DAAF.

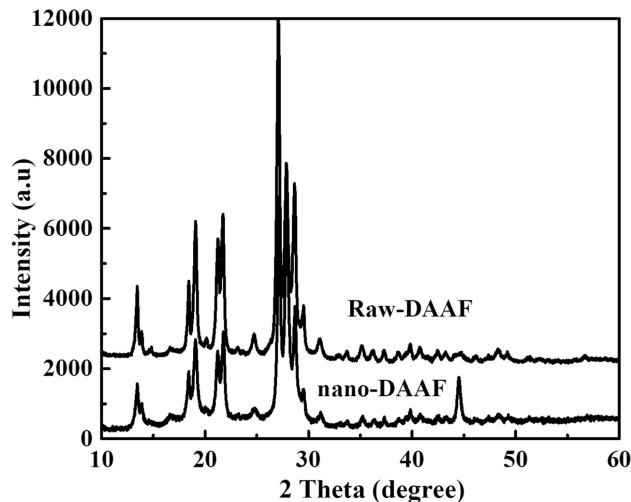


Figure 2. XRD diffraction patterns of the raw- and nano-DAAF.

at $2\theta = 13.14, 18.39, 19.09, 21.21, 21.74, 27.13, 28.68$, and 29.49 are assigned to the (110), (020), (001), (011), (210), (-201), (-211) and (130) reflection lines of the DAAF indicate a high crystallinity. Compared with raw-DAAF, the peaks of nano-DAAF presented in Figure 2, the locations of all peaks were almost unchanged, indicating that the prepared samples are still DAAF. However, when the particle size was reduced to nano-meter range, the peak strength of nano-DAAF in XRD pattern is significantly decreased compared to raw-DAAF. The average size of nano-DAAF can be calculated by inserting the width at half height of the signals into the Debye-Scherer equation. According to Figure 2 and Debye-Scherer equation, the average size of nano-

DAAF is about 63 nm. The calculated size of nano-DAAF is consistent with SEM and AFM results.

According to crystallization process and crystal growth theory, the temperature difference between explosive solvent and water in crystallization process plays an important role in crystal nuclei formation and growth of nano-particles. In order to obtain nano-DAAF with controlled morphology and size, the effect of the temperature difference and concentration of DAAF on the morphology and size of nano-DAAF was investigated carefully. The temperature of water is about 2°C , and solvent is $30, 40, 50$ and 60°C , respectively. The structural evolution of the nano-DAAF is presented in Figure 3a-d. It can be clearly observed that nanoparticles were produced after low-temperature crystallization. Accompanying increasing the solvent temperature (50°C), nano-particles of DAAF with well-distributed size (~100 nm) is formed (Figure 3c). Then the size and morphology further changed after increasing the temperature to 60°C (Figure 3d). The temperature of water is about 2°C , and solvent is 60°C , the effect on size and morphology of DAAF concentration is shown in Figure 3 (d-f). The size of nano-DAAF is reduced with increase of DAAF concentration. The size of nano-DAAF is about 50–60 nm under suitable condition, water is about 2°C , and solvent is 60°C , and saturated DAAF solution. The size and morphology of nano-DAAF changed gradually with increasing solvent temperature and DAAF concentration which reveals the temperature difference and DAAF concentration are important factors for the synthesis of nano-DAAF.

For explosives, thermal property is an important consideration in practical applications. In order to study the influence of nano-DAAF particles on their thermal property, Differential scanning calorimetric (DSC) measurement was carried out. Figure 4 shows DSC curves of DAAF and nano-

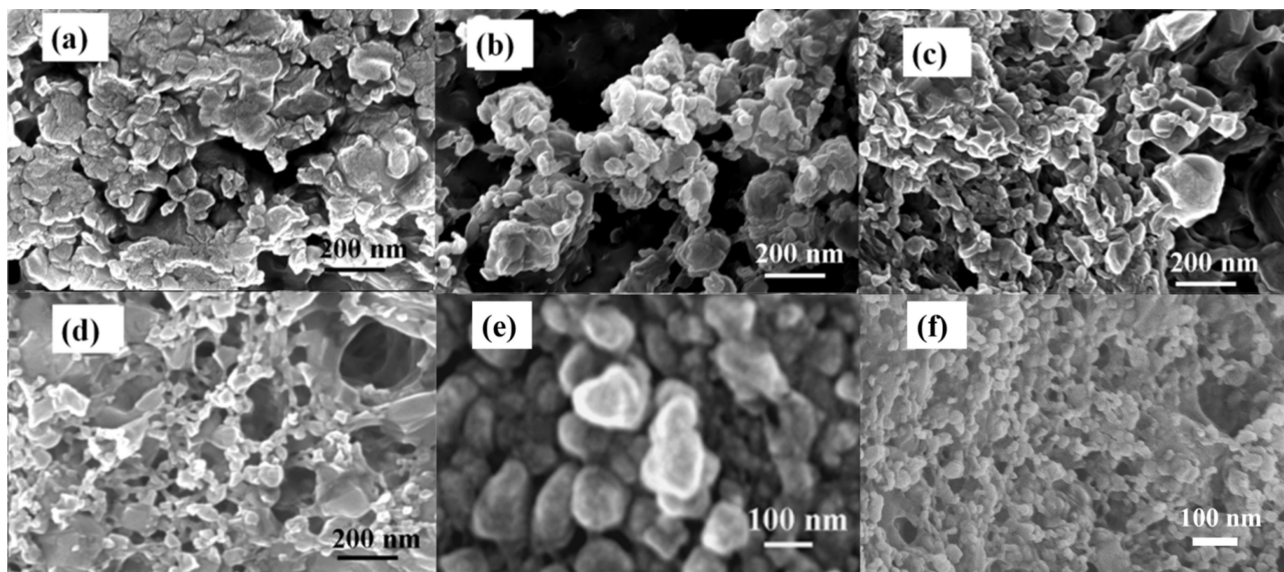


Figure 3. SEM images of nano-DAAF prepared at different temperature and DAAF concentration in crystallization process.

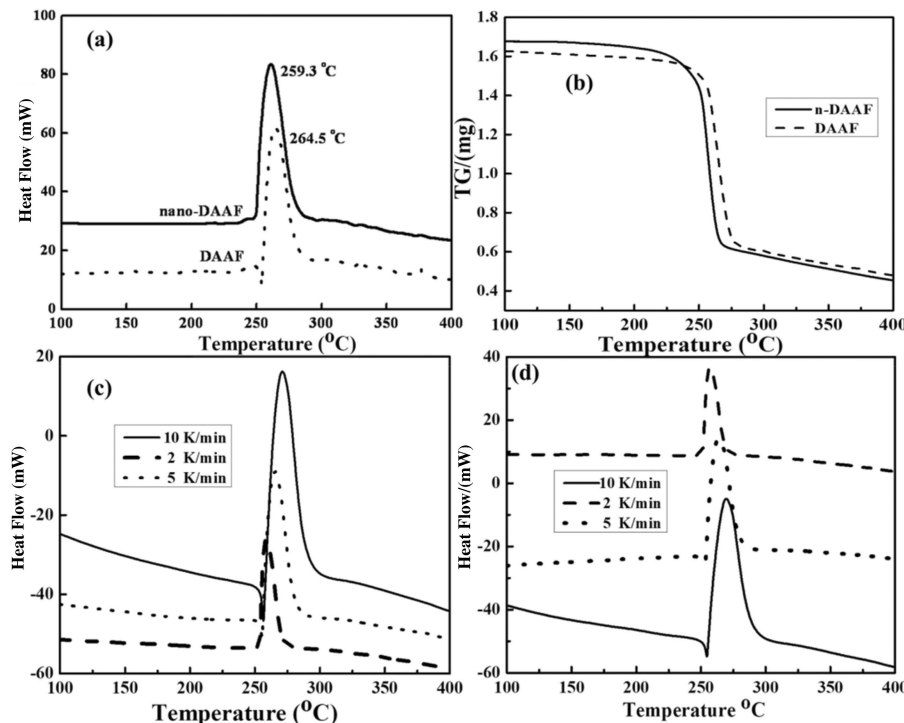


Figure 4. DSC and TG curves of nano-DAAF and DAAF.

DAAF. The exothermal peak occurring at 259 °C of nano-DAAF gradually shift toward a significantly low temperature compared with raw DAAF (264 °C). Activation energy (E_a) and pre-exponential factor (A) of DAAF are calculated based on Kissinger's Eq. For raw-DAAF, the activation energy was calculated to be 215.68 kJ mol⁻¹, however, the activation energy of nano-DAAF decomposition is decreasing to 197.02 kJ mol⁻¹. Furthermore, the value of pre-exponential factor of nano-DAAF is larger than raw-DAAF. The decomposition processes of nano-DAAF were found in a narrow temperature range (248–286 °C) compared with raw DAAF (257–291 °C), which meant that they possessed higher energy release efficiency and significantly improved thermal decomposition kinetics due to size-dependent thermal effect. The total enthalpy of the exothermic peak of nano-DAAF (2771.2 kJ g⁻¹) is higher than raw-DAAF (2321.3 kJ g⁻¹), which further indicates that the nano-DAAF has a higher energy release. The nano-particles with higher surface area have more active reaction sites which are sensitive to the surrounding conditions, including the temperature. The increased surface area and nano-structure can offer more active reaction sites resulting in significantly low decomposed temperature.

Deflagration of DAAF explosive can be illustrated by 5 seconds explosion temperature. The 5 seconds ignition point was determined on the ignition point apparatus by using wood's metal bath method. According to the explosive test method GJB 772A-97-606.1 for the measurement of deflagration point, the 5 seconds ignition point of

the raw-DAAF and nano-DAAF are measured and the results are 224 °C and 216 °C respectively. The explosion temperature of nano-DAAF is lower than that of the raw-DAAF. The possible reason for reduced 5 seconds ignition point is that higher surface area has more active reaction sites and high thermal conductivity of nano-DAAF can promote the heat conduction and reduce the temperature gradient.

Shock initiation is one of the most important properties of explosives for developing modern slapper detonators. In this work, we have used flyer plates to initiate the nano-DAAF and raw-DAAF. Sensitivity towards shock is indicated by flyer velocity of initiation of the samples. For nano-DAAF, flyer velocity of initiation is about 2900 m s⁻¹. However, DAAF can be initiated with the flyer plates with the high speed velocity (3600 m s⁻¹). The results suggest that the nano-DAAF is sensitive to short impulse shock waves and advanced initiating devices.

4 Conclusion

In summary, nano-DAAF was first successfully prepared by using the rapid and low-temperature crystallization process. Nano-DAAF particle displays the shape of near spheres with the diameter ranging from 60 to 100 nm. The temperature difference between explosive solvent and water of crystallization process plays an important role in size and morphology of nano-particles. Nano-DAAF shows significantly low temperature exothermal peak (259 °C) and high energy

release. Nano-DAAF show significantly improved heat and short impulse shock waves sensitivity compare to micro-particles due to high surface area and more active reaction sites. Those results reveal that the nano-DAAF exhibits great potential usage in explosives, solid rocket propellants and advanced initiating devices.

Acknowledgements

This work was supported by the National Natural Science Foundation of China (No. 11502242, and 11502247) and career development funding of CAEP (2402001).

References

- [1] L. Liang, K. Wang, C. Bian, L. Liang, Z. Zhou, 4-Nitro-3-(5-tetrazole) furoxan and Its Salts: Synthesis, Characterization, and Energetic Properties, *Chem. Eur. J.* **2013**, *19*, 14902–14910.
- [2] L. Peng, L. Y. Zhe, Y. T. Tao, L. Jian, Z. W. Zhou, Z. X. Ge, A density Functional theory study on the structure and Thermochemical properties of Azo-bridged Azoles, *Chin. J. Energet. Mater.* **2016**, *24*, 842–847.
- [3] Y. Qu, Q. Zeng, J. Wang, Q. Ma, H. Li, H. Li, G. Yang, Furazans with Azo Linkages: Stable CHNO Energetic Materials with High Densities, Highly Energetic Performance, and Low Impact and Friction Sensitivities, *Chem. Eur. J.* **2016**, *22*, 12527–12532.
- [4] J. Zhang, J. M. Shreeve, 3,3'-Dinitroamino-4,4'-azoxyfurazan and Its Derivatives: An Assembly of Diverse N–O Building Blocks for High-Performance Energetic Materials, *J. Am. Chem. Soc.* **2014**, *136*, 4437–4445.
- [5] L. Wang, C. Yi, H. Zou, Y. Liu, S. Li, Theoretical study on the thermal decomposition mechanism of 3,30-dinitro-4,40-azox-furazan, *Comput. Theor. Chem.* **2011**, *963*, 135–140.
- [6] V. P. Sinditskii, M. C. Vu, A. B. Sheremetev, N. S. Alexandrov, Study on thermal decomposition and combustion of insensitive explosive 3,3'-diamino-4,4'-azofurazan (DAAzF), *Thermochim. Acta* **2008**, *473*, 25–31.
- [7] E. G. Francois, D. E. Chavez, M. M. Sandstrom, The Development of a New Synthesis Process for 3,3'-Diamino-4,4'-azox-furazan (DAAF), *Propellants Explos. Pyrotech.* **2010**, *35*, 529–534.
- [8] D. Chavez, L. Hill, M. Hiskey, S. Kinkead, Preparation and Properties of Azo- and Azoxy-Furazans, *J. Energ. Mater.* **2000**, *18*, 219.
- [9] M. A. Hiskey, D. E. Chavez, R. L. Bishop, J. F. Kramer, S. A. Kinkead, Use of 3,3'-Diamino-4,4'-azoxofurazan and 3,3'-Diamino-4,4'-azofurazan as Insensitive High Explosive Materials, US Patent No. 6358339, **2002**, Washington, D. C.
- [10] E. C. Koch, Insensitive High Explosives II:3,3'-Diamino-4,4'-azoxofurazan (DAAF), *Propellants Explos. Pyrotech.* **2016**, *41*, 526–538.
- [11] Y. Zhang, D. B. Liu, C. X. Lv, Preparation and Characterization of Reticular Nano-HMX, *Propellants Explos. Pyrotech.* **2005**, *30*, 438–453.
- [12] N. Y. Tomoki, K. Makoto, Influences of particle size and content of HMX on burning characteristics of HMX-based propellant, *Aerospace Sci. Tech.* **2013**, *27*, 209–215.
- [13] B. Huang, Z. Qiao, F. Nie, M. Cao, J. Su, H. Huang, Fabrication of FOX-7 quasi-three-dimensional grids of one-dimensional nanostructures via a spray freeze-drying technique and size-dependence of thermal properties, *J. Hazard. Mater.* **2010**, *184*, 561–566.
- [14] D. Kang, J. S. Hwang, M. H. Lee, S. M. Lee, Crystallization and Characterization of HNS-IV for Modern Slapper Detonators, *ICT Konferenz: 34th Int. Annual Conference of ICT*, Karlsruhe, Germany, June 24–27, **2003**, p. 134.
- [15] G. Yang, F. Nie, H. Huang, L. Zhao, W. Pang, Preparation and Characterization of Nano-TATB Explosive, *Propellants Explos. Pyrotech.* **2006**, *31*, 390–395.
- [16] L. Yang, X. Ren, T. Li, S. Wang, T. Zhang, Preparation of Ultrafine TATB and the Technology for Crystal Morphology Control, *Chin. J. Chem.* **2012**, *30*, 293–298.
- [17] J. Wang, H. Huang, W. Zheng, Y. R. Zhang, B. Lu, Prefilming twin-fluid nozzle assisted precipitation method for preparing nanocrystalline HNS and its characterization, *J. Hazard. Mater.* **2009**, *162*, 842–847.
- [18] J. Wang, W. Xu, Effect of Habit Modifiers on Morphology and Properties of Nano-HNS Explosive in Prefilming Twin-Fluid Nozzle-Assisted Precipitation, *Propellants Explos. Pyrotech.* **2009**, *34*, 78–83.
- [19] J. Zhang, P. Wu, Z. Yang, B. Gao, J. Zhang, Preparation and Properties of Submicrometer-Sized LLM-105 via Spray-Crystallization Method, *Propellants Explos. Pyrotech.* **2014**, *39*, 653–657.
- [20] J. Waschl, D. Richardson, Effect of specific surface area on the sensitivity of hexanitrostilbene to flyer plate impact, *J. Energ. Mater.* **1991**, *9*, 269–282.
- [21] Q. F. Fu, M. Li, F. Guo, M. Wang, Y. Wang, Short Duration pulse shock initiation characteristics of ultrafine LLM-105, *Chin. J. Energet. Mater.* **2016**, *24*, 911–914.

Received: March 27, 2018

Revised: July 18, 2018

Published online: September 26, 2018